CFD Letters www.cfdl.issres.net Vol. 4 (1) – March 2012

Numerical Simulation of Buoyant Pulsating Exchange Flow through Circular Opening in Horizontal Partition

B. Gera[c], P. K. Sharma, R. K. Singh, K. K. Vaze
Reactor Safety Division, Bhabha Atomic Research Centre
Trombay, Mumbai, India- 400085

Received: 16/05/2011 – Revised 26/09/2011 – Accepted 14/10/2011

Abstract

An interesting transport phenomenon is observed through openings between two compartments separated by a thin, vented, horizontal partition such as those between containment internals in nuclear power systems, in industrial installations in event of fire, passive cooling of heated structures and in natural building ventilation. A heavier fluid located on the top of a lighter fluid and separated by a horizontal vent constitutes a gravitationally unstable system. Horizontal vents produce flow, which are unstable with irregular oscillatory behavior. The objective of the present work was to simulate such type of flow across a circular opening in horizontal partition in presence of buoyancy force. Unsteady, axisymmetric Navier-Stokes equations have been solved with Finite Volume Method. The equations were solved using the in-house CFD code based upon the well-established pressure-based finite volume methodology. In terms of temporal differencing second order accurate Crank-Nicolson scheme was used. Interpolation to cell faces for the convective terms was performed using a third order QUICK scheme, second order central differencing was used for the viscous terms. Pressure-velocity coupling was based on the SIMPLE procedure. The upper chamber was filled with salt water and the lower chamber with fresh water, creating a density differential between the two chambers. Opposing forces at the interface created a gravitationally unstable system, and an oscillating exchange of fluid developed. Three different cases for vent length to diameter ratio (L/D) 0.008, 0.0376 and 0.106 from a reported experiment were examined. The pulsation frequencies and their decay with time have been determined. The flow coefficients were computed and compared with experimental results.

Keywords: salt water; horizontal partition; CFD; oscillation; circular opening.

1. Introduction

The buoyancy driven exchange flow through the large openings in horizontal partitions occurs in many practical situations. Mixing processes in large enclosures by buoyancy driven fluid motion through vents are important in many applications. The density difference between two compartments arises partly due to difference in composition and partly from the difference in temperature. Vents in horizontal partition are important in many situations particularly in multiple

[c] Corresponding Author: B. Gera
Email: bgera@barc.gov.in Telephone: +91-22-25595158 Fax: +91-22-25505151

PII: S2180-1363(12)4120-X

room compartments and nuclear containment buildings. Flow through opening in horizontal partition is unstable, turbulent and bi-directional. Several experiments and numerical studies have been performed to characterize such type of flow through such large openings. A lot of research has been done to study buoyancy driven exchange flow across the opening using salt water/fresh water. Since it is difficult and very expensive to do study with full-scale model, therefore salt water/fresh water experiment is not only an effective way but also an economical approach to study this mixing phenomenon. The liquid system has its advantage over a gas filled system in performing a heat transfer experiment: there is no need to cover the test section with insulation as the density driven flow is isothermal and flow visualization is very easy.

Brown and Solvason [1] conducted one of the earliest studies on countercurrent exchange flow. It was determined that the exchange flow rate is affected by the thickness of the partition and it increases with increase in L/D ratio. Using air as the fluid medium, results were obtained for 0.0825<L/D<0.66. Epstein [2] started to study buoyancy driven exchange flow through opening using salt water/fresh water. The bottom enclosure was filled with fresh water and the top with salt water separated by a horizontal partition having vent. Based on mass balance of upper and lower compartment following equation for flow rate Q (m^3/s) from the upper compartment to lower compartment was developed.

$$Q(t) = \frac{-V_H (d\rho_H / dt)}{(\rho_H - \rho_{L,0}) - \frac{V_H}{V_L}(\rho_{H,0} - \rho_H)} \tag{1}$$

Where V_H, V_L are the volumes, ρ_H, ρ_L are the densities and $\rho_{H,0}$, $\rho_{L,0}$ are the initial densities of upper and lower compartment respectively. It was found that for a given aspect ratio the volumetric exchange flow rate at any instant is proportional to

$$Q_s(t) \equiv \sqrt{\frac{D^5 g \Delta\rho(t)}{\rho(t)}} \text{ or} \tag{2}$$

$$Q^* = \frac{Q(t)}{Q_s(t)} \tag{3}$$

Where $\Delta\rho(t)$ is the instantaneous density difference between the two enclosures and $\rho(t)$ is the instantaneous average of these two densities, $Q_s(t)$ is the instantaneous scale flow rate and Q^* is the flow coefficient. The exchange flow was defined as the minimum flow from either enclosure to the other necessary to account for the observed transport of salt from top enclosure to the bottom. This flow rate is equal to the upward or downward flow rate at the horizontal partition cross section. Four different flow regimes were defined namely regime 1: oscillatory exchange flow regimes for 0.01<L/D<0.16, regime 2: Bernoulli flow regimes for 0.16<L/D<0.4, regime 3: combined turbulent diffusion and Bernoulli flow for 0.4<L/D<1.32 and regime 4: turbulent diffusion for 1.32<L/D<20. Epstein and Kenton [3] extended the earlier work [2] for multiple openings in the horizontal partition. The flow through openings was observed unidirectional and forms the convective loop. On the other hand, simultaneous unidirectional flow and bi-directional flows were also observed. Jaluria et al. [4] studied the combined pressure and density driven flow across the horizontal vent using salt water/fresh water. Provision was made to pressurize the bottom compartment by injecting more fresh water. Photographs of shadowgraph images were recorded to study transition from bi-directional to unidirectional flow as pressure difference increases. Tan and Jaluria [5] did the same experiment as [4] at higher pressure of lower compartment and found purging or flooding pressure at which there is only unidirectional flow in upward direction. Shadowgraph images were captured of simultaneous bi-directional flow that converted into unidirectional as pressure of bottom compartment increases. The results can be applied for prediction of fire growth in the compartment. Linden et al. [6] have used salt water/fresh water to study natural ventilation flow through vent in horizontal partition. Kuhn et al. [7] have performed experimental study of transient density stratification from buoyancy driven and forced convection flows through horizontal partitions in a

liquid tank. Two openings in horizontal partition were provided at different position and a unidirectional convective loop was obtained. Two hot film probes used to measure the exchange flow rate were installed below the openings. Conover et al. [8] studied the oscillatory exchange flow across the horizontal opening for small L/D ratio. Three different vent length-to-diameter ratios 0.008, 0.0376 and 0.106 were studied, the nature of oscillation was measured with LDV and shadowgraph for flow visualization and frequencies of oscillations were identified. Velocity measurements were made in the water plume in the upper compartment using a 2D three beam LDV system. To visualize the flow shadowgraph images ware recorded by a standard VHS video camera. A pulsating exchange flow was observed across the opening. Gera [9] has studied the oscillatory bi-directional flow through opening in horizontal partition with salt water/fresh water. The oscillation was captured with shadowgraph and salt concentration along the plume was monitored with electric conductivity probes [10].

Apart from experiments various analytical and numerical computation have been performed to find the oscillatory nature of flow through opening in horizontal partition separating heavier fluid at the top with lighter fluid in the bottom enclosure. A numerical study of unsteady buoyant flow through a horizontal vent placed slightly asymmetrically between two enclosed vents was performed by Singhal and Kumar [11]. A numerical investigation of countercurrent flow exchange through a vent in horizontal partition is performed by Spall and Anderson [12] for an infinitesimally thin partition. Harrison and Spall [13] studied numerically effects of axisymmetric partition thickness on counter current flow with water as the fluid medium. They concluded that the flow exchange increases with increasing partition thickness over the range of $0.0376 \leq L/D \leq 0.3$, and decreases in the range of $0.3 \leq L/D \leq 1$. In all studies discussed above, only high Rayleigh number ranges were investigated so that the effect of viscosity could be neglected and in general, flow coefficient was determined as a function of L/D. The 2D numerical simulation was carried out by Sleiti [14] for such type of flow at low Rayleigh number. The flow exchange between enclosures for L/D = 0.5, 1 and 2 was studied with air as fluid medium. Similarly various numerical and analytical simulations have been performed for oscillatory exchange flow through opening in horizontal partition with air as fluid medium slightly overheated in lower enclosure compared to upper enclosure [15-19].

Most of earlier numerical studies for buoyant pulsating exchange flow through circular opening in horizontal partition have been carried out with air as fluid medium. Only very few studies have been reported with water as fluid medium but flow has been considered as laminar. However if salt water/fresh water is considered as the fluid medium the corresponding Rayleigh number is high that suggest that the flow itself is turbulent. In the present paper the authors have reported use of in-house buoyancy modified turbulent CFD code for buoyant pulsating exchange flow through circular opening in horizontal partition of small thickness. Three different opening aspect ratio 0.008, 0.0376 and 0.106 as used by Conover et al. [8] have been studied numerically. The frequency of oscillation was found and decay of pulsation frequency and density of upper compartment was also computed. The flow coefficient as suggested by Epstein [2] was numerically computed and compared with experimental results for validation of the code. The paper briefly describes some of the details of the experiment, salient features of the CFD numerical model and results of the computation carried out for buoyant pulsating exchange flow through circular opening in horizontal partition with salt water/fresh water.

2. General Description of the Problem

The geometry was chosen from the experimental setup of Conover et al. [8]. The setup consisted of two compartments separated by horizontal partition plate was made of transparent material for ease in flow visualisation. The lower compartment was 0.381 m square by 0.316 m high. The upper compartment was 0.381 m square by 0.265 m high. An insertion plate with a 0.127 m dia hole at the centre was sealed to the partition plate by an O-ring. Holes 0.0508 m (2 inches) in

diameter were served in plates of varying thickness to be used as vents. Velocity measurements were made in the water plume in the upper compartment using a 2-D three beam laser Doppler velocimetry system. The experiments were conducted with three different opening aspect ratio (L/D) 0.008, 0.0376 and 0.106 with initial salt water density as 1011.5, 1012.75 and 1012 kg/m^3. The operating range of Reynolds number was 4650-2685 during the experiments which suggests that the flow was turbulent for such type of flow.

3. Numerical details

A sketch of the simplified geometric configuration used for CFD computation is shown in figure 1. To simplify the numerical computation a cylindrical geometry was chosen, the compartment diameter was evaluated so that the compartment volume remains same as was in the experiments. The simulations were carried out with 2D axisymmetric assumption. The geometry consisted of a cylinder of radius (R) 0.215 m and height 0.316 (H_2) and 0.265 m (H_1) of lower and upper chambers respectively separated by a thin partition, containing a hole of diameter (D) 0.0508 m (2 inches).

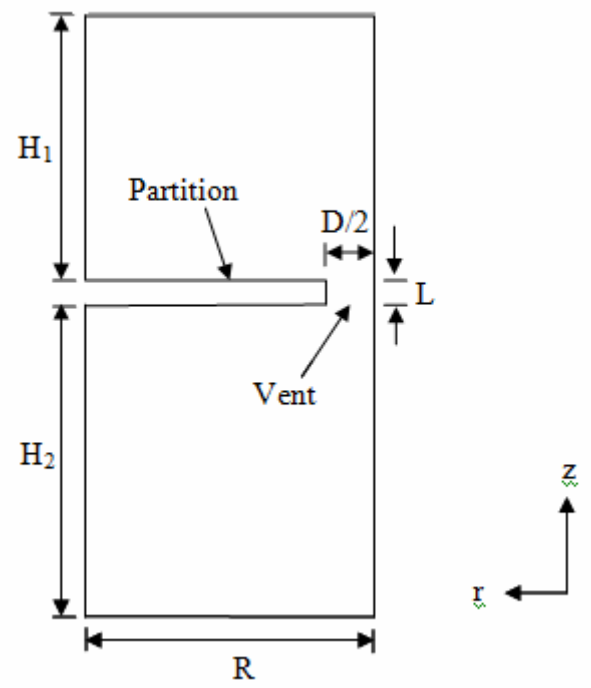

Figure 1. Simplified geometric configuration for CFD computation: A cylindrical tank separated by a thin horizontal partition having circular vent

3.1. Governing equations

The governing equations for fluid flow, turbulence and species transport are as follows. The general transport equation for variable ϕ is

$$\frac{\partial(\rho\phi)}{\partial t}+\frac{\partial(\rho u\phi)}{\partial z}+\frac{1}{r}\frac{\partial(r\rho v\phi)}{\partial r}=\frac{\partial}{\partial z}(\Gamma_\phi\frac{\partial\phi}{\partial z})+\frac{1}{r}\frac{\partial}{\partial r}(r\Gamma_\phi\frac{\partial\phi}{\partial r})+S_\phi \qquad (4)$$

where ρ is density of mixture (kg/m^3), t is time (s), u, v are axial and radial component of velocity (m/s), z, r are axial and radial coordinate direction, Γ_Φ is diffusion coefficient for variable ϕ and S_ϕ is source term for variable ϕ.

For continuity ϕ = 1 and S_ϕ=0.

For Z-momentum $\phi = u$ and $\Gamma_\phi = \mu_{eff} = \mu + \mu_t$ and

$$S_\phi = -\frac{\partial p}{\partial z} + \frac{\partial}{\partial z}(\mu_{eff}\frac{\partial u}{\partial z}) + \frac{1}{r}\frac{\partial}{\partial r}(r\mu_{eff}\frac{\partial v}{\partial z}) - (\rho - \rho_{ref})g \quad (5)$$

Where μ is dynamic viscosity (Ns/m^2), μ_t is turbulent viscosity, μ_{eff} is effective viscosity, p is dynamic pressure and g is acceleration due to gravity (9.81 m/s^2).

For R-momentum $\phi = v$ and $\Gamma_\phi = \mu_{eff} = \mu + \mu_t$ and

$$S_\phi = -\frac{\partial p}{\partial r} - \frac{2}{r^2}\left(\mu_{eff} v\right) + \frac{\partial}{\partial z}(\mu_{eff}\frac{\partial u}{\partial r}) + \frac{1}{r}\frac{\partial}{\partial r}(r\mu_{eff}\frac{\partial v}{\partial r}) \quad (6)$$

For species transport $\phi = Y$ and $\Gamma_\phi = \rho D + \mu_t / Sc_t$ and S_ϕ=0. Where Y is mass fraction of species, D is diffusion coefficient, Sc_t is turbulent Schmit number.

For modelling the turbulence, realizable $k-\varepsilon$ model developed by Shih et al. [20] has been used with standard wall function and buoyancy modification. Where k is turbulent kinetic energy (m^2/s^2) and ε is turbulent dissipation rate (m^2/s^3). This $k-\varepsilon$ model is distinct from the standard $k-\varepsilon$ model in terms of the determination of empirical constant C_μ and the transport equation for the turbulent dissipation rate. The former guarantees the realizability of the model while the latter solves the problem of the plane jet-round jet anomaly (i.e. the fact that the standard $k-\varepsilon$ model accurately predicts the spreading rate of a planar jet but strongly over predicts the spreading rate of a round jet). For the realisable $k-\varepsilon$ model the turbulent viscosity is modelled as

$$\mu_t = \rho C_\mu \frac{k^2}{\varepsilon} \quad (7)$$

For turbulent kinetic energy $\phi = k$, $\Gamma_\phi = \mu + \mu_t / \mathrm{Pr}_k$ and

$$S_\phi = G_k + G_B - \rho\varepsilon \quad (8)$$

Where Pr_k is turbulent Prandtl number for kinetic energy, G_k is generation term for turbulent kinetic energy due to the mean velocity gradients and G_B is generation term for turbulent kinetic energy due to buoyancy, calculated in same way as standard $k-\varepsilon$ model.

For turbulent dissipation rate $\phi = \varepsilon$, $\Gamma_\phi = \mu + \mu_t / \mathrm{Pr}_\varepsilon$ and

$$S_\phi = \rho C_1 S\varepsilon - \rho C_2 \frac{\varepsilon^2}{k + \sqrt{\upsilon\varepsilon}} + \frac{\varepsilon}{k} C_3 G_B \quad (9)$$

Where Sc_t , Pr_k , Pr_ε , C_1 , C_2 and C_3 are empirical coefficients whose standard values were taken, Pr_ε is turbulent Prandtl number for dissipation

$$G_k = \mu_t \{2[(\frac{\partial u}{\partial z})^2 + (\frac{\partial v}{\partial r})^2 + (\frac{v}{r})^2] + (\frac{\partial u}{\partial r} + \frac{\partial v}{\partial z})^2\} \quad (10)$$

And the term G_B has been modelled by Simple Gradient Diffusion Hypothesis (SGDH)

$$G_B = -\frac{\mu_t}{\mathrm{Pr}_t}\frac{1}{\rho^2}\frac{\partial \rho}{\partial z}(\frac{\partial p}{\partial z} + \rho_{ref} g) \quad (11)$$

In the equation (11) it has been assumed that the pressure gradient is negligible. Assuming the pressure gradient negligible is reasonable due to the fact that the plume velocity is relatively low creating low pressure gradients. In equation (9) representing the source term for transport equation of ε; Viollet [21] has adopted the following procedure for determining the value of C_3 based on the sign of G_B; the term denoting the buoyancy production of turbulence. If G_B > 0;

C_3 = 1.44 and C_3 = 0 if G_B < 0. The sign of G_B is related to the stability of flow. If G_B > 0; the flow is unstable since $\partial\rho/\partial z$ > 0 and, if G_B < 0; the flow is stable $\partial\rho/\partial z$ < 0. Where

$$C_1 = \max(0.43, \frac{\eta}{\eta+5}) \ , \ \eta = S\frac{k}{\varepsilon} \ , \ S = \sqrt{2S_{ij}S_{ij}}$$

In realisable $k-\varepsilon$ model C_μ is not constant and is computed from

$$C_\mu = \frac{1}{A_0 + A_s\frac{kU^*}{\varepsilon}} \qquad (12)$$

Where

$U^* = \sqrt{S_{ij}S_{ij} + \tilde{\Omega}_{ij}\tilde{\Omega}_{ij}}$ and $\tilde{\Omega}_{ij} = \overline{\Omega}_{ij} - \varepsilon_{ijk}\omega_k - 2\varepsilon_{ijk}\omega_k$

In the above equation, $\overline{\Omega}_{ij}$ is the mean rate of rotation tensor viewed in a rotating reference frame with angular velocity ω_k. The constants A_0 and A_S are defined as;

$$A_0 = 4.04 \ , \ A_S = \sqrt{6}\cos\phi$$

Where

$$\phi = \frac{1}{3}\cos^{-1}(\sqrt{6}\frac{S_{ij}S_{jk}S_{ki}}{\tilde{S}^3}) \ , \ \tilde{S} = \sqrt{S_{ij}S_{ij}} \ , \ S_{ij} = \frac{1}{2}(\frac{\partial u_j}{\partial x_i} + \frac{\partial u_i}{\partial x_j})$$

It has been shown that C_μ is a function of the mean strain and rotational rates, the angular velocity of the rotating system, and the turbulent kinetic energy and its dissipation rate. The standard value of C_μ = 0.09 is found to be the solution of equation (12) for an inertial sub layer in the equilibrium boundary layer. The constants C_2 , Pr_k , Pr_ε and Sc_t have been determined by Shih et al. [20] and are defined as C_2=1.9, Pr_k =1.0, Pr_ε =1.2 and Sc_t =0.7. Inclusion of the production term due to buoyancy in the $k-\varepsilon$ model was first proposed by Rodi [22].

3.2. Solver details

The axisymmetric, incompressible, unsteady momentum, species, turbulence and continuity equations were solved using the in-house computational fluid dynamics (CFD) code based on the well-established pressure-based finite-volume methodology using Patankar's SIMPLE algorithm [23]. Interpolation to the cell faces for the convective terms was performed using a third-order QUICK scheme suggested by Hayase et al. [24]. Second-order central differencing was used for the diffusive terms. A second-order-accurate Crank-Nicolson scheme was used for the temporal differencing.

At time zero seconds the density of the water in the upper chamber was set to salt water density and that of the lower chamber was set to fresh water density. Resulting relevant dimensionless parameters include the density ratio $\Delta\rho/\bar{\rho}$ = 1.2%, and, a densimetric Reynolds number (Re) = 4,560, values which are in the range of those used by Conover et al. [8]. The fluid was assumed initially quiescent and therefore the velocity components were initialized to zero. The cylindrical wall and partition has been modelled as no-slip wall. The mixture density has been modelled as volume weighted mixing law. Staggered scheme of solution was used in which fluid velocities were calculated at cell face and scalars such as pressure, species mass fraction and turbulent quantities were evaluated at cell centre. The equations were iteratively solved using Gauss-Seidel method. A low value of under-relaxation was used to have easy convergence since the solutions were oscillating nature. Under-relaxation was set as 0.05 for momentum and 0.1 for other equations. The convergence criterion was set 10^{-5} based on overall mass residual. Each simulation required approximately 20 hrs run time on a P-IV machine with 4GB RAM for 3000 second of problem run. A temporal discretization of 0.1 s was used for final runs. A temporal discretization of 0.05 s was also employed to assess temporal convergence.

However, the smaller time step resulted in nearly identical results; consequently 0.1 s was determined to be adequate. 100 internal iterations were used per time step, which was sufficient to limit the residuals errors. A non-uniform grid system was employed for mesh generation. The y^+ was in the range of 30-80 near the walls which is required to use standard wall function. In axial direction grid was made fine near partition and made coarser away from the partition. In radial direction uniform grid was employed upto opening region after that grid was made non-uniform coarser towards outer radius. To achieve grid independent results four different number of grids were tested and their effect on flow coefficient was observed. The grids used were 82 X 70, 210 X 140, 300 X 210 and 400 X 280 in axial and radial direction respectively. Figure 2 shows the results of the grid refinement study done for the opening aspect ratio 0.008 used in the present work.

It clearly shows that flow coefficient have a monotonic increase in the value and approach a limiting value as the grid size is increased. An examination of the flow coefficient indicates that the grid size 210 X 140 is sufficiently fine to obtain results that are essentially grid independent. Initial conditions corresponding to zero velocity were set, however density difference creates instability at interface small perturbation is required to start the oscillating flow. The transition of the flow from a steady to an unsteady condition is automatically initiated by computer round-off errors, thus eliminated the need to perturb the solution.

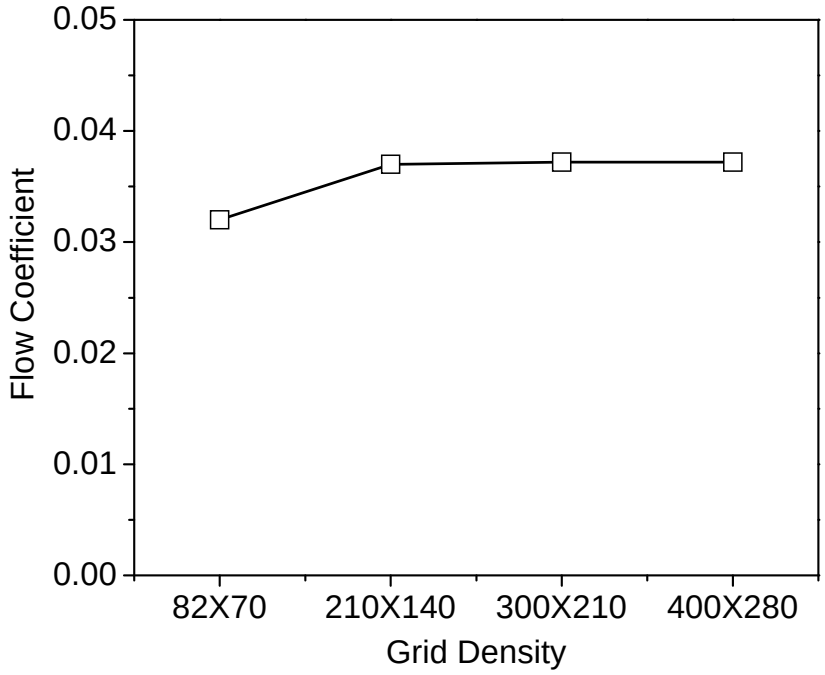

Figure 2. The mesh size sensitivity exercise results for L/D=0.008

4. Results and discussion

The results were evaluated in terms of flow coefficient, pulsation frequency and their decay with time for all three L/D ratio. Figure 3 depicts the numerically obtained flow coefficient using equation (2)-(3) and their comparison with Conover et al. [8], two more case were studied for L/D=0.015 and 0.028 for comparison with Epstein [2] and shown in same figure as a part of validation exercise. The difference in value may be attributed to the procedure used for evaluation of flow coefficient. During experiments the actual flow rate was calculated from equation (1), for this, flow was stopped after regular intervals, then upper compartment was stirred and density of upper compartment was measured. Thus the decay of density of upper compartment was evaluated by closing the opening at regular intervals and stirring the upper compartment. But in numerical

simulation the exchange flow rate is directly available from computation thus the upper compartment was not homogenized after regular interval. The theoretical flow rate was calculated by equation (2) during numerical simulation as well as experimental procedure.

The flow coefficient is plotted in figure 3 for each of the opening aspect ratio and represents an averaged value over the time span 200 seconds. The initial time level of 200 seconds was chosen to exclude transients during the start-up phase. The flow coefficient increases linearly with L/D. Density ratio $\Delta\rho/\bar{\rho}$ has an influence on flow coefficients. For L/D 0.015 and 0.028 where comparison with Epstein [2] experiments is shown in figure 3 the density ratio $\Delta\rho/\bar{\rho}$ was 4% while for comparison with Conover et al. [8] experiments the initial density ratio was maintained 1.2%. The high value of the driving potential gives high value of the flow coefficient. The flow coefficient is a function of driving potential $\Delta\rho/\bar{\rho}$ and L/D. For same $\Delta\rho/\bar{\rho}$ flow coefficient increases linearly upto L/D=0.6. The flow coefficient is maximum ad L/D=0.6 as reported in previous studies. The flow rate through opening location is governed by driving potential $\Delta\rho/\bar{\rho}$ and viscous resistance based on length of opening. At high L/D viscous resistance is more hence the flow coefficient has a low value, while at low L/D the velocity magnitude in opposite direction is high. This increases the turbulence due to high shear but reduces the effective transfer of fluid from one compartment to another. At lower L/D flow rate decreases and appears to be tending towards a constant value [2].

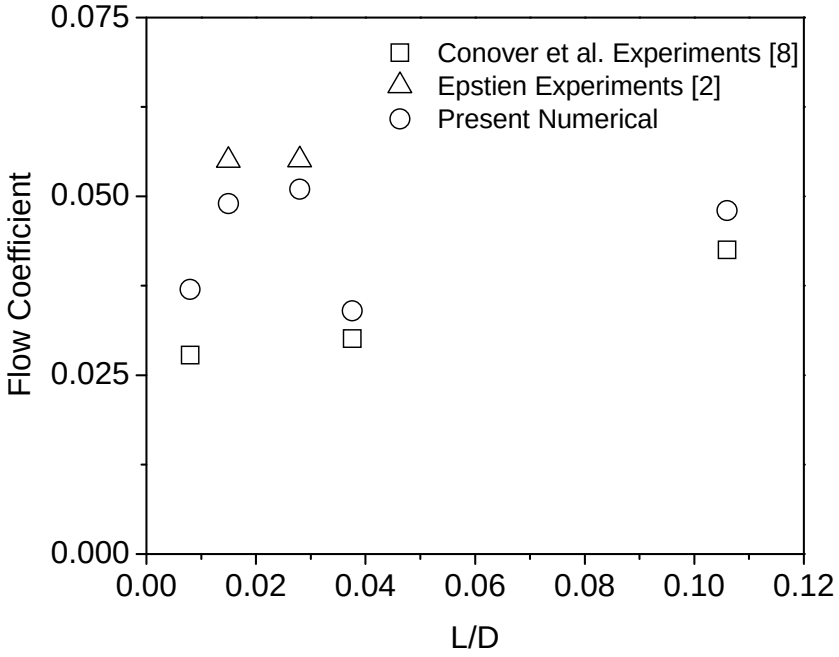

Figure 3. Comparison of numerically determined flow coefficients with the experiments

The numerically obtained flow coefficients as a function of time for L/D=0.0376 are shown in figure 4. The numerically obtained values have been compared with reported experiment and numerical results in same figure. The results reveal that through 2000 seconds the flow coefficients are nearly constant. The variation of density of upper compartment is depicted in figure 5 for all the three cases and compared with experimental results of Conover et al. [8]. The flow coefficient is maximum for L/D=0.106 hence fluid is transferred at a faster rate and therefore approaches the equilibrium density value more rapidly. At very small L/D the pressure at the interface is essentially the same in both the compartment. But the interface is unstable because a heavy density fluid is lying over lower density fluid. Thus a small random perturbation may initiate a pulsating exchange flow through the opening. This is the result of “Taylor instability” that the flow exchange takes place from one compartment to another. This exchange flow is pulsating in nature and these pulsations are characterized by oscillatory nature of vertical velocity component at opening

location. To capture the pulsation frequency the vertical velocity component was monitored at various points at opening location as a function of time. The variation of local axial velocity with time at opening centre location for L/D=0.008 is shown in figure 6.

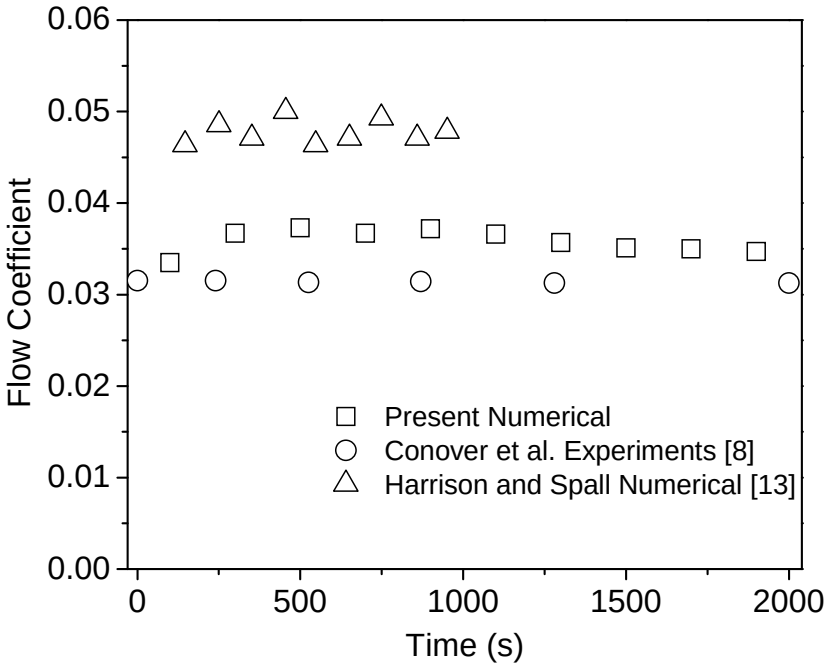

Figure 4. Variation of flow coefficient for L/D=0.0376 with time

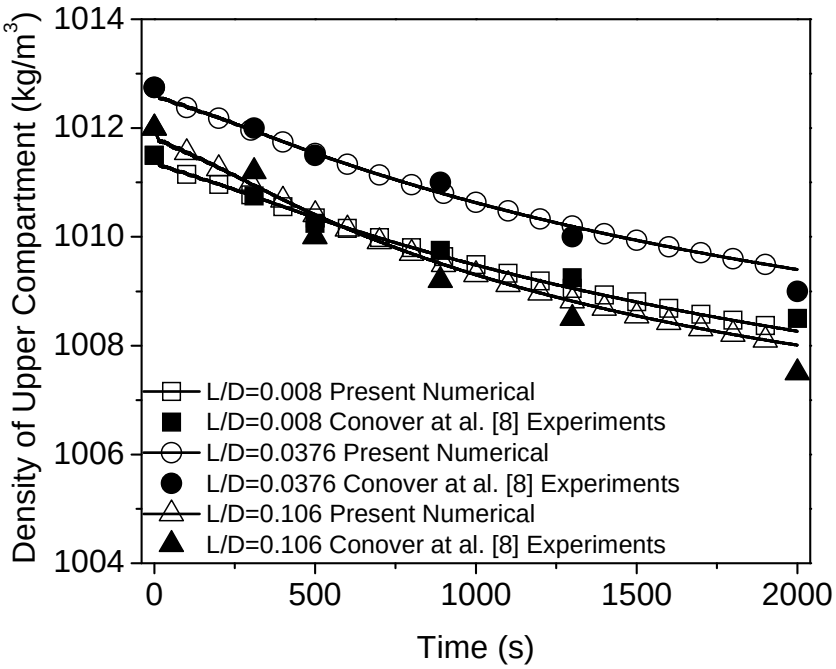

Figure 5. Variation of upper compartment density with time for all three cases

A random oscillatory pattern was observed that consist of various frequencies. The FFT analysis has been performed to evaluate the existence of dominant pulsation frequency. The power spectra were computed using the vertical component of velocity taken at a point near the centre of the vent. The FFT analysis performed for all the cases are shown in figure 7. The figure 7 clearly indicates the existence of two prominent frequencies for L/D=0.008. These results are in accord with the experimental results presented by Conover et al. [8]. In that work, two dominant

frequencies were observed for the lowest aspect ratio case studied, L/D=0.008, whereas for higher L/D, only a single dominant frequency appeared. The variation of high and low pulsation frequency with time for L/D=0.008 is shown in figure 8.

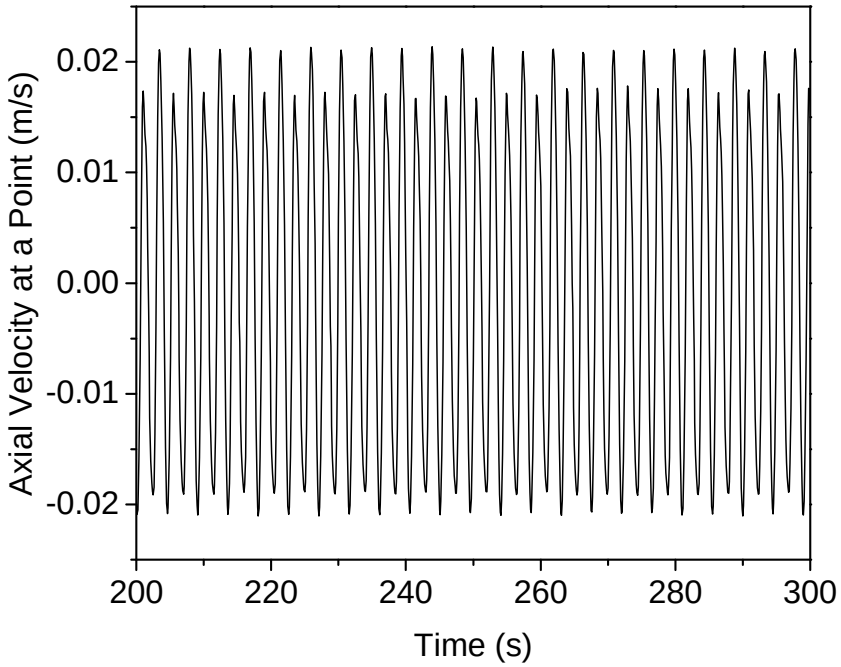

Figure 6. Axial velocity at the centre of opening location for L/D=0.008

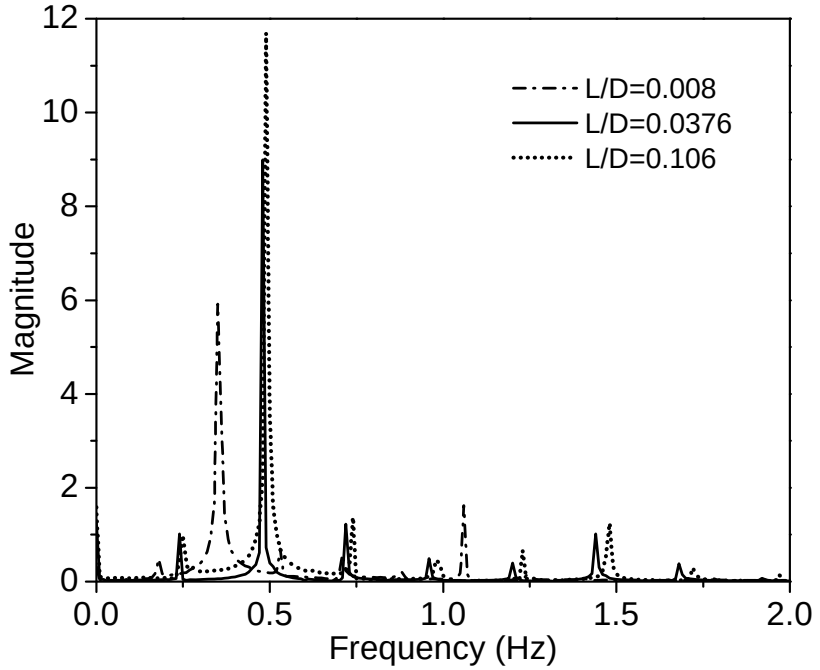

Figure 7. Typical FFT analysis results for L/D=0.008, 0.0376 and 0.106

As the density of salt water decays the driving potential decreases thus the frequency decreases. The higher frequency for L/D=0.008 decreases very fast as compared to lower frequency. The lower frequency corresponds to exchange flow and higher frequency corresponds to formation of secondary ripples in the circumferential direction at the interface as suggested by Conover et al. [8]. The decay pattern of pulsation frequency for L/D=0.0376, 0.106 and low frequency for

L/D=0.008 is compared in figure 9. The decay of pulsation frequency is much faster for L/D=0.106 as compared to L/D=0.0376.

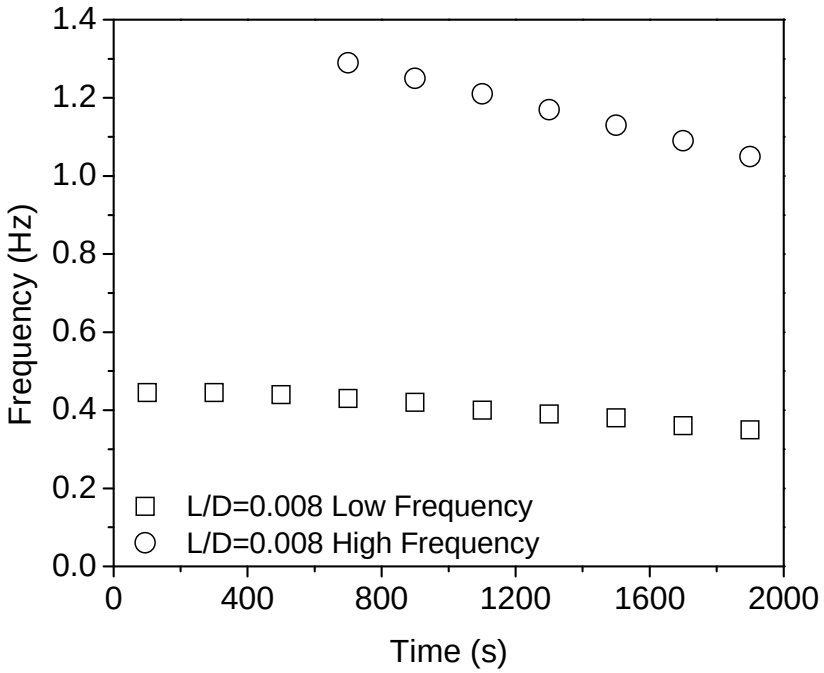

Figure 8. Decay of pulsation frequencies for L/D=0.008

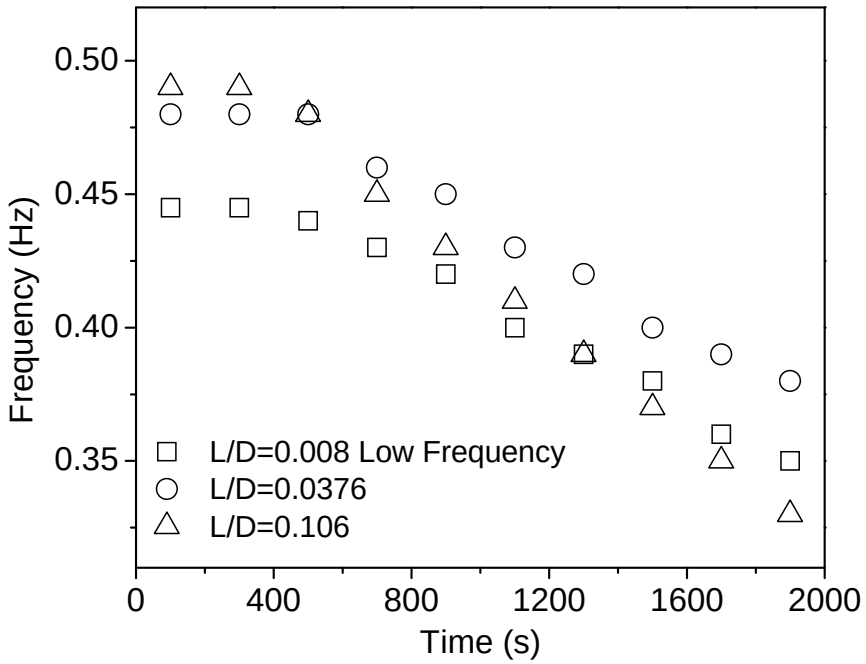

Figure 9. Decay of pulsation frequencies for L/D=0.008, 0.0376 and 0.106

5. Conclusion

Numerical computations have been performed for buoyant pulsating exchange flow through horizontal circular opening in a partition between two compartments. The flow coefficient was calculated and compared with reported experimental results. The flow coefficients were in good agreement with experimental prediction. The pulsation frequency and their decay with time were also found from numerical results. Two dominant frequencies were identified for L/D=0.008. The

present study was limited for $L/D \leq 0.106$, basically in the oscillatory exchange flow regime as suggested by Epstein [2]. The computation for higher L/D ratio could be considered in future.

References

[1] Brown, W.G. and K.R. Salvason, *Natural convection through rectangular openings in partitions-2: horizontal openings.* International Journal of Heat and Mass Transfer, 1962. **5**: p. 869-880.

[2] Epstein, M., *Buoyancy driven exchange flows through small opening in horizontal partitions.* Journal of Heat Transfer, 1988. **110**: p. 885-893.

[3] Epstein, M. and M.A. Kenton, *Combined natural convection and forced flow through small opening in horizontal partitions, with special references to flow in multicompartment enclosures.* Journal of Heat Transfer, 1989. **111**: p. 980-987.

[4] Jaluria, Y., S.H.K. Lee, G.P. Mercier and Q. Tan, *Transport processes across a horizontal vent due to density and pressure differences.* Experimental Thermal and Fluid Science, 1998. **16**: p. 260-273.

[5] Tan, Q. and Y. Jaluria, *Mass flow through a horizontal vent in an enclosure due to pressure and density differences.* International Journal of Heat and Mass Transfer, 2001. **44**: p. 1543-1553.

[6] Linden, P.F., G.F. Law-Serff and D.A. Smeed, *Emptying filling boxes: the fluid mechanics of natural ventilation.* Journal of Fluid Mechanics, 1990. **212**: p. 309-335.

[7] Kuhn, S.Z., R.D. Bernardis, C.H. Lee and P.F. Peterson, *Density stratification from buoyancy driven exchange flow through horizontal partition in a liquid tank.* Nuclear Engineering and Design, 2001. **204**: p. 337-345.

[8] Conover, T.A., R. Kumar and J.S. Kapat, *Buoyant pulsating exchange flow through a vent.* Journal of Heat Transfer, 1995. **117**: p. 641-648.

[9] Gera, B., *Investigation of bi-directional flow behaviour of a large opening*, M. Tech Thesis 2005, Department of Mechanical Engineering, IIT Delhi, India.

[10] Gera, B., P.K. Sharma, M.R. Ravi and A.K. Ghosh, *Fresh-salt water experimental studies for buoyant flow behaviour in large vertical and horizontal ceiling opening.* in *2005 Proceedings of the 16th Annual Conference of Indian Nuclear Society*, November 15-18, 2005. BARC Mumbai, India.

[11] Singhal, M. and R. Kumar, *Unsteady buoyant exchange flow through a horizontal partition.* Journal of Heat Transfer, 1995. **117**: p. 515–520.

[12] Spall, R.E. and E.A. Anderson, *A numerical study of buoyant, pulsating exchange flows through a vent in a thin horizontal partition.* Numerical Heat Transfer Part A, 1999. **36**: p. 263–272.

[13] Harrison, R.P. and R.E. Spall, *The effect of partition thickness on buoyant exchange flow through a horizontal opening.* Numerical Heat Transfer Part A, 2003. **44**: p. 451-462.

[14] Sleiti, A.K., *Effect of vent aspect ratio on unsteady laminar buoyant flow through rectangular vents in large enclosures.* International Journal of Heat and Mass Transfer, 2008. **51**: p. 4850–4861.

[15] Kerrison, L., E.R. Galea and M.K. Patel, *A two dimensional investigation of the oscillatory flow behaviour in rectangular fire compartment with a single horizontal ceiling vent.* Fire Safety Journal, 1998. **30**: p. 357-382.

[16] Cooper, L.Y., *Calculating combined buoyancy and pressure driven flow through a shallow, horizontal, circular vent.* Fire Safety Journal, 1996. **27**: p. 23-35.

[17] Chow, W.K. and Y. Gao, *Oscillating behaviour of fire-induced air flow through a ceiling vent.* Applied Thermal Engineering, 2009. **29**: p. 3289–3298.

[18] Tan, Q. and Y. Jaluria, *Flow through horizontal vents as related to compartment fire environments.* 2007. NIST-GCR-92-607.

[19] Mishra, A.A., H. Nadeem, S. Sanghi and R. Kumar, *Two-dimensional buoyancy driven thermal mixing in a horizontally partitioned adiabatic enclosure.* Physics of Fluids, 2008. 20:063601.

[20] Shih, T.H., W.W. Liou, A. Shabbir, Z. Yang and J. Zhu, *A new k-ε eddy viscosity model for high Reynolds number turbulent flows.* Computers & Fluids, 1995. **24**: p. 227-238.

[21] Viollet, P.L., *The modeling of turbulent recirculating flows for the purpose of reactor thermal-hydraulic analysis.* Nuclear Engineering and Design, 1987. **99**: p. 365–377.

[22] Rodi, W., *Turbulence Models, Their Application in Hydraulics-a State of Art Review.* 1978. University of Karlsruhe, SFB/80/T/127.

[23] Patankar, S.V. Numerical Heat Transfer and Fluid Flow. Hemisphere Pub. Co. Washington, DC, 1980.

[24] Hayase, T., J.A.C. Humphrey and R.A. Grief, *Consistently formulated QUICK scheme for fast and stable convergence using finite volume iterative calculation procedures.* Journal of Computational Physics, 1992. **98**: p. 108–118.